JGR Oceans

RESEARCH ARTICLE
10.1029/2020JC016472

Water Mass Variability and Levantine Intermediate Water Formation in the Eastern Mediterranean Between 2015 and 2017

Bettina A. Fach[1], Hasan Orek[1], Elif Yilmaz[1], Devrim Tezcan[1], Ilkay Salihoglu[2], Baris Salihoglu[1], and Mohammed Abdul Latif[1]

[1]Institute of Marine Sciences, Middle East Technical University, Erdemli, Turkey, [2]University of Kyrenia, Maritime Transportation and Management Engineering, Kyrenia, TRNC

Key Points:

- Seasonal cruise data show that Levantine Intermediate Water (LIW) formation caused by intense cooling occurs in the Cilician Basin
- A significant increase in salinity by 0.5 is observed in Levantine Surface Waters and by 0.11 in LIW over the 2.5 years study period
- The circulation in the region is dominated by meso-scale, short-lived eddies with life spans of a few months

Supporting Information:

- Supporting Information S1

Correspondence to:
B. A. Fach,
bfach@ims.metu.edu.tr

Citation:
Fach, B. A., Orek, H., Yilmaz, E., Tezcan, D., Salihoglu, I., Salihoglu, B., & Latif, M. A. (2021). Water mass variability and Levantine Intermediate Water formation in the Eastern Mediterranean between 2015 and 2017. *Journal of Geophysical Research: Oceans*, *126*, e2020JC016472. https://doi.org/10.1029/2020JC016472

Received 5 JUN 2020
Accepted 11 JAN 2021

Abstract The physical characteristics of water masses in the Cilician Basin were analyzed based on recent, comprehensive in-situ data. Nine seasonal cruises from June 2015 to November 2017 were carried out in an area located in the north-eastern Levantine Basin between the coasts of Turkey and Cyprus. In this little studied area, the structure of the water column, its seasonal variability, and water formation events are investigated. The extensive data set reveals that in summer Modified Atlantic Water (MAW) is observed at about 50 m depth. Saltier and warmer Levantine Intermediate Water (LIW) lies below the MAW between ~100 and 250 m. During winter, the water column becomes mixed due to surface cooling and vertical convection, and displays uniform properties from the surface to about 200–300 m depths. The yearly cycle of a vertically uniform water column during winter and the appearance of LIW in the following period suggests that LIW is being formed in this region, which is confirmed through heat and buoyancy flux calculations. It is the first time LIW formation is reported in this area of the north-eastern Levantine Basin and adds to the areas of LIW formation outside Rhodes Gyre. In the 2.5 years of the study, LIW salinity increased by 0.11 psu in 2017, while surface water salinity increased by 0.5 psu over the same period. The presence of meso-scale eddies in the study area is observed throughout the year. The eddies are short-lived, having a time span of a few months, during which they either change location or disappear.

Plain Language Summary Variability of water mass properties in the Cilician Basin, located in the north-eastern part of the Mediterranean Sea, was investigated during nine research cruises spanning 2.5 years. This was done measuring temperature, salinity, and oxygen of the water column at several locations in the region. The study describes the seasonal cycle of the water masses and it is shown for the first time that in winter cold, dense water is formed in this region that sinks to depths of 100–250 m. This is because water increases its density due to cooling and forms a water mass known as Levantine Intermediate Water. It is of importance to know where and how much of this water mass is formed, because it travels throughout the Mediterranean Sea and exits through the Strait of Gibraltar, where it influences the water masses and circulation in the Atlantic Ocean. The study also found that the salinity of that water mass increased by 0.11 psu in 2017, while at the same time surface water salinity increased by 0.5 psu. This is a large increase over a short time compared to the long term 0.0007 ± 0.0003 psu/yr average increase calculated for the Mediterranean Sea in previous studies.

1. Introduction

The circulation and water masses of the Eastern Mediterranean have been comprehensively investigated in the past decades, particularly during the multi-national POEM and LIWEX programs (Malanotte-Rizzoli et al., 1999, 2003; Robinson et al., 1992). However, the region of the north-eastern Levantine Basin between the coasts of Turkey and Cyprus, the Cilician Basin, has been studied only in a very limited manner in the past. In the present study, the seasonal variability of the water masses in the Cilician Basin is studied for the first time systematically over the course of 2.5 years with nine seasonal cruises.

The Mediterranean Sea is an evaporative basin, with a net annual loss of about 70 cm/yr (Mariotti et al., 2002; Tanhua et al., 2013). This deficit is compensated by the inflow from the Atlantic Ocean through the Strait of Gibraltar. The general circulation in the north-eastern Levantine Basin comprises of the Mid-Mediterranean

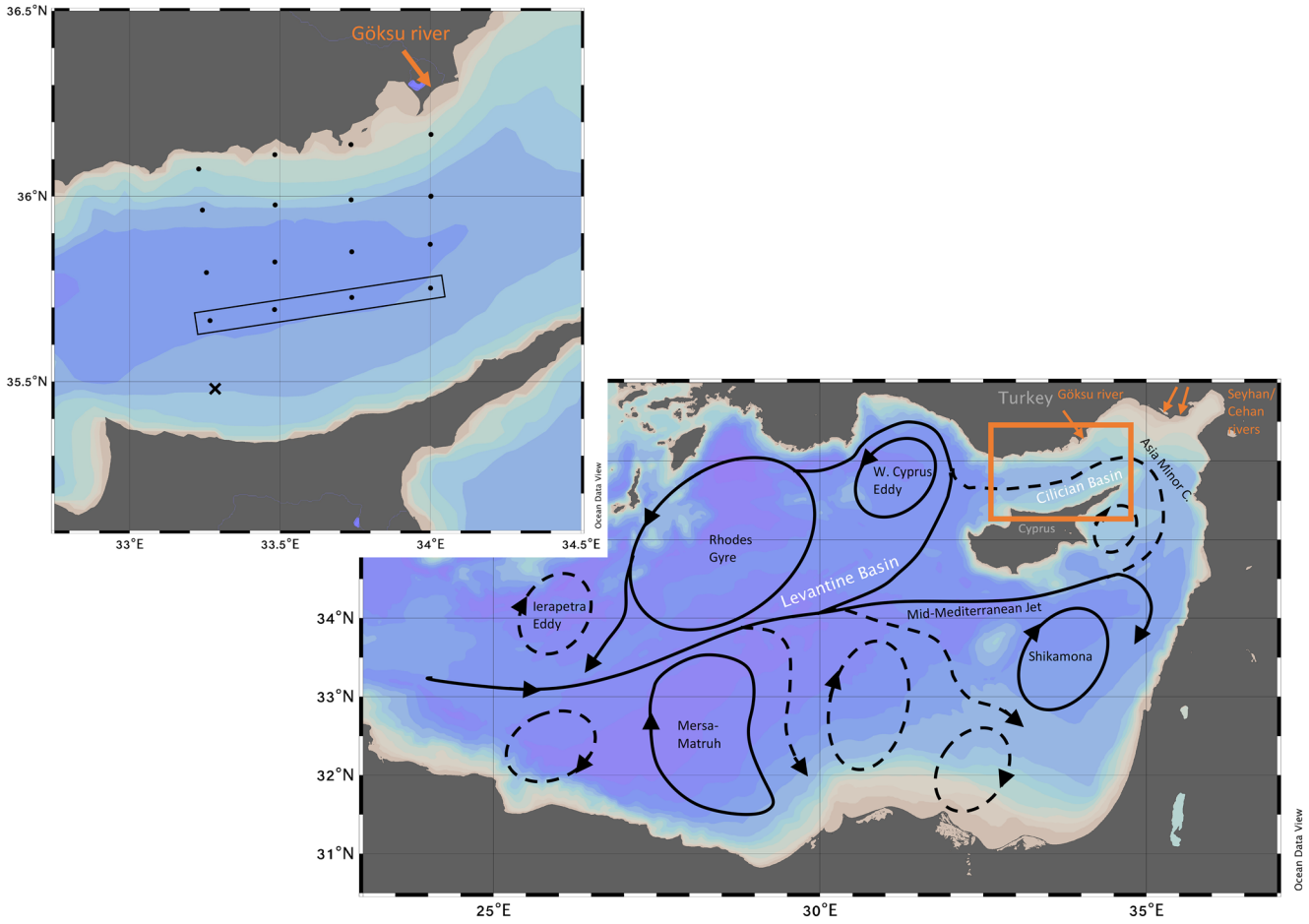

Figure 1. Location of the study area in the Cilician Basin with station locations of the seasonal cruises (black dots) and the location of the ECMWF atmospheric data (x). The rectangle marks the transect along which data in Figures 2 and 5 are drawn. The study region is inset in a representation of the Levantine Basin general circulation redrawn after Robinson et al. (1992). Orange arrows show the location of the Göksu River inside the orange box marking the study region and the Seyhan and Cehan rivers to the east of the study region.

Jet (MMJ) that moves from south of Rhodes Gyre eastward to the south of Cyprus, where it bifurcates and the northern branch turns into the Asia Minor Current (AMC), circling the northern tip of Cyprus and flowing westward in the Cilician and Antalya Basins (Figure 1). The AMC contributes to the flow in this region with its meanders and mesoscale eddies spinning off it (Ozsoy et al, 1991, 1993; Robinson, 2001).

The regional climate is marked by hot, humid summers, and mild winters. However, the interaction of atmospheric systems with coastal mountain ranges considerably influences the atmospheric conditions in the region. The north-eastern Levantine Basin is surrounded by the steep Taurus and Amanos mountains which have narrow coastal plains, interrupted by the river deltas of the Seyhan, Ceyhan, and Göksu rivers (Figure 1). In winter and spring, the winds are predominantly northerly due to the Poyraz and Sirocco winds (Ozsoy, 1981; Ozsoy et al., 1989). In winter, the northerly, cold, and dry (locally known as Poyraz) winds blow through the river valleys and gaps in the Taurus mountains along the Turkish coast for long time periods (Ozsoy, 1981; Ozsoy et al., 1989). These winds have a high cooling and evaporating potential and lead to strong buoyancy loss events that can cause the formation of Levantine Intermediate Water (Malanotte-Rizzoli et al., 2003; Morcos, 1972; Ozsoy et al., 1993; Wüst, 1961). Therefore, the northern margin of the Levantine Basin is a possible region for LIW formation apart from the Rhodes Gyre, which is the hypothesis explored in this study.

The basin-scale circulation of the Mediterranean Sea is driven by surface inflow of Atlantic Water from the Atlantic Ocean through the upper ~50m at the Strait of Gibraltar (Sannino et al., 2014; Tanhua et al., 2013)

with a salinity of ~36.15 and temperature of ~15°C. After passing the western Mediterranean basin the Atlantic water continues its eastward flow in the eastern basin, thereby increasing in salinity and temperature (Malanotte-Rizzoli & Bergamasco, 1989; Malanotte-Rizzoli & Hecht, 1988; Pinardi & Masetti, 2000; Wüst, 1961) due to the strong evaporation in this basin. It is then called Modified Atlantic Water (MAW) with a salinity of ~38.6 and can be observed as far as the eastern boundary of the Levantine Basin at depths of 50–150 m depth (Ozsoy et al., 1981). Together with highly saline (>39 psu) and warm (~28°C) Levantine Surface Water (LSW), it is known to play an important role in the formation of Levantine Intermediate Water.

LIW originating in the Levantine Basin is located below MAW and forms a return flow toward Gibraltar (Malanotte-Rizzoli et al., 2014). It comprises approximately 26% of the total water volume of the Mediterranean Sea (Ovchinnikov, 1984). The renewal time of the LIW has been calculated to be 26 years, meaning that 4% of its total volume is renewed annually (Ovchinnikov, 1984). LIW flows westward across the entire basin in the opposite direction to the inflowing MAW, but not along the same path, and eventually exits the Mediterranean at the Strait of Gibraltar at intermediate depths (Malanotte-Rizzoli et al., 2014; Tanhua et al., 2013; Wu and Haines, 1998).

LIW forms when highly saline LSW cools during winter convection events. The consequent increase in density results in mixing and sinking of the surface waters. In the Eastern Mediterranean, the LIW formation process generally begins with the onset of the cooling season in November. Ultimately by February/March the surface layer, which is highly oxygenated, becomes denser than the underlying water and sinks to intermediate depths depending on formation location (ca. 130–350 m) (Hecht et al., 1988; Ozsoy et al., 1989). In a T-S diagram, LIW is seen as an increase in salinity at intermediate depths, also called "scorpion tail." At depths of 800 m and below, the Eastern Mediterranean Deep Water (EMDW) is located. LIW has been observed to form mainly in the Rhodes Gyre area (Ozsoy et al., 1989), however it has also been reported that LIW formation can occur in cyclonic eddies of the Asia Minor Currents during extreme cooling events, such as in the Gulf of Antalya (Kubin et al., 2019; Ozsoy et al., 1989; Sur et al., 1992) and east of Antalya due to the interaction of the boundary current with the vorticity dynamics (Waldmann et al., 2018).

The process of LIW water formation, is of interest because it allows the exchange of physical and biochemical properties (e.g., oxygen, nutrients) between the surface and deeper layers, while retaining its characteristics caused by environmental conditions specific to the formation site. LIW exits the Mediterranean Sea from the Strait of Gibraltar (Malanotte-Rizzoli et al., 2014; Tanhua et al., 2013; Wu & Haines, 1998) and its signature is clearly seen in the Atlantic Ocean, influencing the salinity content there. Hence the formation process in the Levantine Basin and any variability therein has wide reaching implications, even outside the Mediterranean. It is therefore of particular interest if LIW formation takes place in the Cilician Basin, in locations outside the Rhodes Gyre, adding to the volume of intermediate deep water produced in the Levantine Basin.

Hence, the main aim of this study is to examine the temporal and regional variations of the water mass properties in the Cilician Basin, with particular emphasis on exploring the possibility of LIW formation. This is accomplished by analyzing an unprecedented, extensive data set of temperature, salinity and dissolved oxygen from nine seasonal cruises between July 2015 and November 2017, which is analyzed in conjunction with atmospheric data and historical cruise data.

2. Data and Methods

Nine seasonal cruises were carried out between July 2015 and November 2017 by R/V BILIM-2 operated by the Institute of Marine Sciences of Middle East Technical Institute (IMS-METU). The cruises took place in July and November 2015, February, April, July, and October 2016, and February, July, and November 2017. Data were collected at 16 stations in the Cilician Basin (Figure 1). Station locations varied slightly between cruises and at times not all stations could be covered due to weather conditions. In total, 148 CTD profiles were collected. A Seabird SBE 911 plus CTD system with a rosette of 24 Niskin bottles was used until March 2016 when it was lost on a cruise in a different area. Its sensors were calibrated in May 2014. From March 2016 on another Seabird SBE 911 plus CTD was then used, the sensors were

calibrated in February 2016. The CTD data were quality checked following SBE and Seadatanet protocols. Oxygen was measured with a dissolved oxygen sensor (SBE 43) during all cruises. Water samples taken at all stations and at discrete depths were used to measure dissolved oxygen using the Winkler titration method (Carpenter, 1965) and an intercalibration between the oxygen sensors was performed. It was found that the sensor readings drifted slightly over time and linear regression was applied to the oxygen sensor data to correct this drift.

Furthermore, data from the November 1985 and April 1986 cruises of R/V Bilim-2 in the northern Levantine Basin are presented in this study (see Figure 10). These data were collected within the framework of the POEM project and have been previously published (Malanotte-Rizzoli et al., 2003; Robinson et al., 1992).

Atmospheric data such as heat flux, wind, and evaporation in the area are evaluated to determine the effects of solar radiation and atmospheric variation on the water column properties. These data are downloaded from European Center for Medium-Range Weather Forecasts (ECMWF) ERA-Interim daily data set between dates 10/2014 to 03/2018. The closest grid point to station A03 (Figure 1) is chosen to compare with CTD data collected during the cruises. Heat flux (Joules), radiation (Joules), and evaporation (mm) data are accumulative variables so daily total values are calculated. 10-m wind speed (m/s) is an instantaneous variable so first daily averaged values are calculated before the magnitude and direction of the wind speed. Total air-sea heat exchange across the surface is calculated from the formulation

$$Q_{\text{total}} = Q_s - Q_b - Q_h - Q_e \tag{1}$$

which considers the net shortwave solar radiation (Q_s, the difference between downward and reflected solar radiation) minus surface net thermal radiation (Q_b longwave) surface latent heat flux (Q_e) and surface sensible heat flux (Q_h).

To understand the impact of heat loss in the study region, the surface buoyancy per unit area B_0 ($m^2\ s^{-3}$) is calculated following Mertens and Schott (1998) using both heat and freshwater fluxes:

$$B_0 = g\left[\alpha\left(c_p\rho_0\right)^{-1}Q_t - \beta S_0\left(E - P\right)\right] \tag{2}$$

Here g is the gravity acceleration, α is the thermal expansion coefficient, c_p is the specific heat, ρ_0 is the reference density of seawater (1,029 kg m^{-3}), Q_t is the total surface heat flux described above in Equation 1, β is the expansion coefficient for salinity (value computed for 100m), S_0 is a typical surface salinity, and E and P evaporation and precipitation rates. The terms $(E–P)$ and Q_t are calculated from the EMCWF Era Interim atmospheric data described above.

In addition, the total buoyancy content of the water column is calculated from CTD data with respect to a reference density ρ_0 following Zahariev and Garrett (1997) where the change of the buoyancy content in time $B(t_1)$–$B(t_2)$ can be related to the total buoyancy flux B_{tot}. The total buoyancy content can be calculated as follows:

$$B\left(t\right) = \int_{-D}^{0} -g\rho_0^{-1}\left[\rho\left(t,z\right) - \rho_0\right]dz \tag{3}$$

with D being the depth until which the value is integrated, taken as the base of the mixed water column (200 m).

Finally, the general surface circulation features in the Cilician Basin are examined using absolute dynamic topography (ADT) generated by the SSALTO/DUACS delayed time altimeter data at a 0.125 × 0.125-degree resolution. Daily nighttime sea surface temperature (SST) data at a 0.05 × 0.05-degree resolution generated from AVHRR data are also used in this study. Both data sets are distributed by the E.U. Copernicus Marine and Environment Monitoring Service (CMEMS) (http://www.marine.copernicus.eu). In addition, quality-controlled Argo float data were downloaded from the Ifremer Data Assembly Center (ftp://ftp.ifremer.fr/ifremer/argo/dac/coriolis/) and analyzed.

3. Results

3.1. Water Masses in the Cilician Basin

In this section, the data collected in four of the nine cruises are discussed. These four cruises were chosen to be from the first year of the study and are representative of the seasonal dynamics observed during the study. The vertical distribution of salinity, potential temperature, dissolved oxygen and potential density anomaly from summer 2015-spring 2016 (Figure 2) are taken along the transect marked in Figure 1. The stations covered in each cruise vary slightly, depending on weather conditions and sometimes instrument

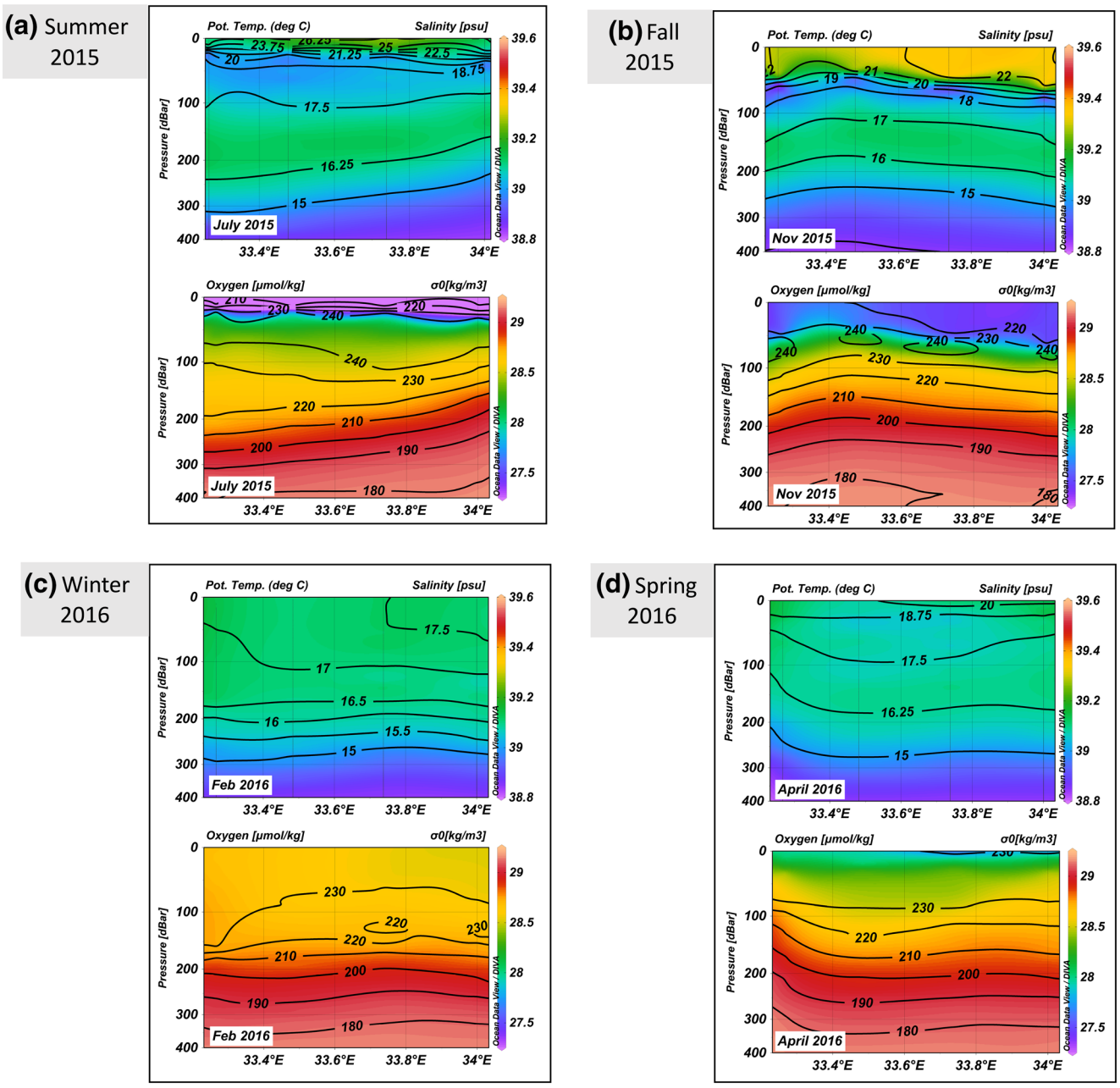

Figure 2. Results of the first four cruises starting in (a) summer 2015, (b) Fall 2015, (c) Winter 2016, and (d) Spring 2016. For each of the four cruises the following data are shown along the transect indicated in Figure 1: Upper panel—Potential temperature versus depth transect (black contour lines) overlaid over salinity versus depth transect (color shading). Lower panel—Dissolved oxygen versus depth transect (black contour lines) overlaid over potential density anomaly versus depth (color shading). In all figures, the upper part of the water column is stretched to better illustrate the changes in the first 200 m.

problems. This transect was chosen as being representative of the general distribution of these properties, since it contains most of the measurements. Although measurements were generally taken to 1000 m or to the bottom at shallower stations, the plots are given to a depth of 400 m to be able to focus on the features in the upper part of the water column. Information on the latter five cruises can be found in Figure S1.

The 2015 summer cruise, carried out between June 30 and July 1, shows the presence of the typical water masses in the eastern Mediterranean Sea in this season. At the surface, temperatures reach 26°C and salinity 39.25 psu (Figure 2a). The mixed layer is about 25 m deep. MAW is located at about 50 m depth. LIW, identified by 39.12 psu salinity and 28.8 kg/m^3 density, is located at depths between 100 and 200 m along the entire length of the section and trends upwards toward the eastern part of the section. The oxygen section shows that the surface layer is saturated with oxygen, as it is in contact with the atmosphere. There is a subsurface oxygen maximum that stems from high ventilation in winter that has been topped by less oxygenated water and retains its values from the winter. Such a shallow oxygen maximum is generally found centered around 50 m in the Eastern Mediterranean (Manca et al., 2004) and is a well-known feature of the MAW, corresponding to the low salinity of the MAW. It is also observed in the fall cruise.

Data from the fall cruise 2015, carried out on November 17–18, about three and a half months after the July cruise, shows a drop of about 5°C in the sea surface temperature (Figure 2b). The water column is mixed to 50 m depth because of vertical convection induced by cooling and wind mixing. There are no significant changes in the position and the properties of the MAW and LIW water masses (Figure 2b). The oxygen section shows that the surface layer is still saturated with oxygen and the shallow oxygen maximum continues to be centered at approximately 50 m.

In the winter 2016 cruise, carried out on February 8–9, the effect of continued cooling and vertical convection in the intervening period of about 3 months since the November cruise is observed. The LIW and MAW at depth are not observed because the mixed layer has deepened to about 200–250 m (Figure 2c). The upward doming of the temperature isolines and density isopycnals, and the high values of oxygen, about 220 μmol/kg, corresponding to 92% saturation, show that ventilation of the surface layer is taking place, resulting in further cooling and increase in density. This is the process of LIW formation. Similar features are present in other sections in the study region as well and the doming of isopycnals is even more pronounced in February 2017 (see Supporting Information S1C). This process may occur elsewhere in the Levantine basin during winter-early spring and is also found in the south-eastern Lazarev Sea (Lazar, 2019).

In spring, during the April 2016 cruise taking place April 18–19, the effect of warming is starting to be seen in the form of higher potential temperature in the water column with potential temperature up to 20°C at the surface (Figure 2d). Because of the warming of surface waters, the presence of LIW is now seen at a depth of 100–200 m, with a 39.1 salinity and 28.75 kg/m3 density. The oxygen content is high in the upper 100 m and has increased to 234 μmol/kg at the surface compared to 220 μmol/kg in winter.

3.1.1. Influence of River Inflow

The Mediterranean Sea is an evaporative basin and river inflow into the basin is relatively low. In the north-eastern Levantine Basin though there are four rivers discharging into the sea, namely the Ceyhan and Seyhan Rivers, close to Adana, and the Göksu and Lamas rivers near the study region in the Cilician Basin (see Figure 1). Of these rivers the Ceyhan, Seyhan and Göksu rivers have significant yearly water discharge of 7.18, 8.01, and 0.31 km^3/year respectively, as reported by Akbulut et al. (2009). The main discharge of the Göksu river occurs in the months January to May (Ediger et al., 1997).

In the study region, the influence of the Göksu river was not detectable, except for stations near the coast. In summer 2015 and in spring 2016, one coastal station showed slightly fresher surface waters (around 39.0 psu) (Figure 4). The influence of the river inflow therefore does not reach far into the study region, but is limited to the coastal region and to a depth of about 50 m (Figure 3). The offshore stations, specifically the transect along which above data was shown (see Figure 1), is unaffected by fresh water from river inflow.

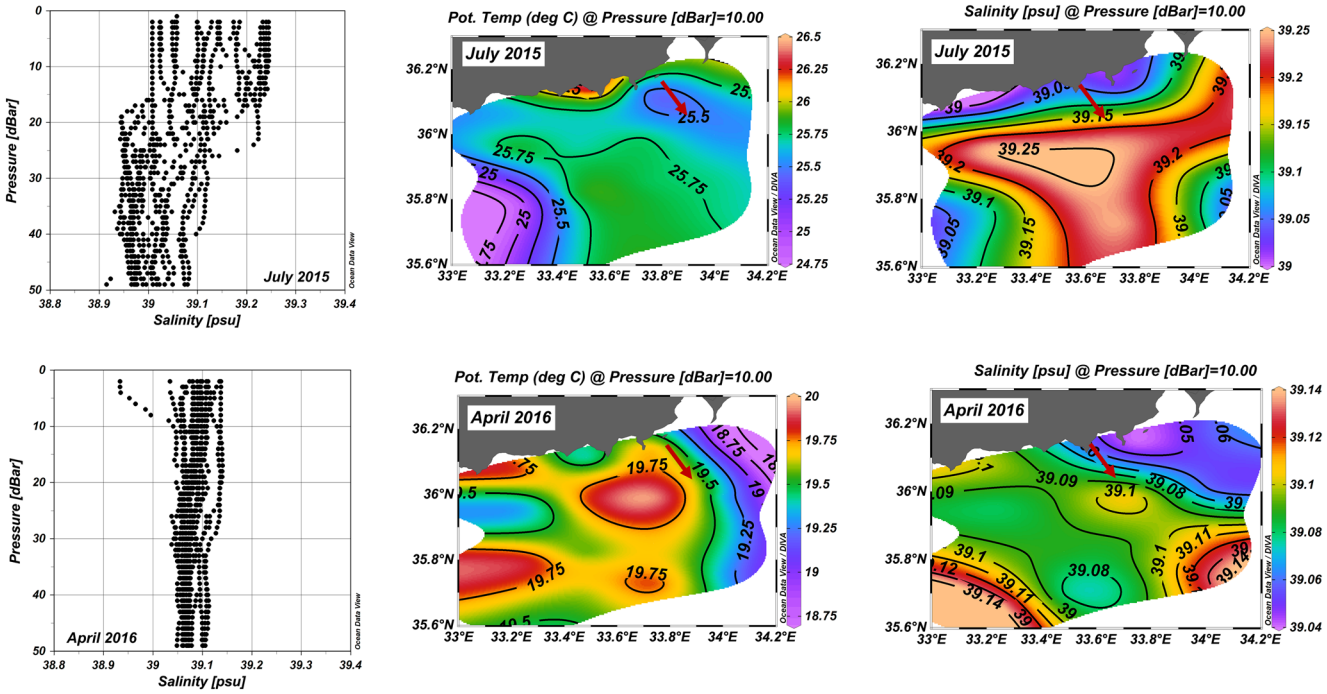

Figure 3. Depth profiles of salinity at all stations (left), as well as potential temperature (middle) and salinity (right) maps of the study area at 10 m in July 2015 (top row) and April 2016 (bottom row).

3.2 Properties of LIW in the Cilician Basin

Potential temperature-salinity (T-S) diagrams depict the temporal evolution of the water masses during the cruises in the Cilician Basin (Figure 4). There is a progression of the water column from a stratified state in summer to a homogeneously mixed state (to a depth of about 300 m) in winter. Since the sections in Figure 2 encompass only four or five stations, we here include data of all stations for each cruise in the T-S diagrams to better illustrate the annual cycle of the transformation of the water column in the entire region.

The T-S plot of the first cruise in July 2015 (Figure 4a) has a typical shape for the summer season in this region. The surface layer, the MAW and LIW situated below and the beginning of the EMDW at about 800–900 m are clearly defined as is the typical "scorpion tail" form. In November 2015 (Figure 4b), the effect of surface cooling and the consequent deepening of the surface mixed layer (see Figure 2b) is seen. However, the MAW and LIW remain essentially unchanged. In the following cruise, in February 2016, the water column becomes thoroughly mixed (Figure 4c) down to ~200–250 m (Figure 2c) due to continued cooling and vertical convection in the period since the November cruise. However, below the LIW, the transition zone between LIW and EMDW is not affected by the mixing, as the waters below are of higher density. This T-S diagram shows the process of LIW formation, when much of the water column is mixed and the T-S profile is confined to potential temperature of below 17.1 C, salinity below 39.2 psu and sigma t below 28.77 km m^{-3}. During the April 2016 cruise carried out about two and a half months later, LIW is found at about 170 m (Figure 4d). LIW is not as clearly defined then as in the fall season, because only a slight recapping of the surface layer has occurred (see also Figure 2d). The summer 2016 cruise data of July (Figure 4e) are strikingly similar to the July 2015 cruise data (Figure 4a). Once again, the surface layer, MAW, and LIW are clearly defined. In the remaining four cruises, carried out in October 2016 and in February, July, and November 2017 (Figures 4f–4i) the cycle described above is repeated. The seasonal cycle, particularly the erosion of the high salinity LIW though mixing of the water column to ~200–250 m in winter followed by the reappearance of LIW after the February cruises, is a strong indication of local LIW formation. It is indicating that water transported into the region

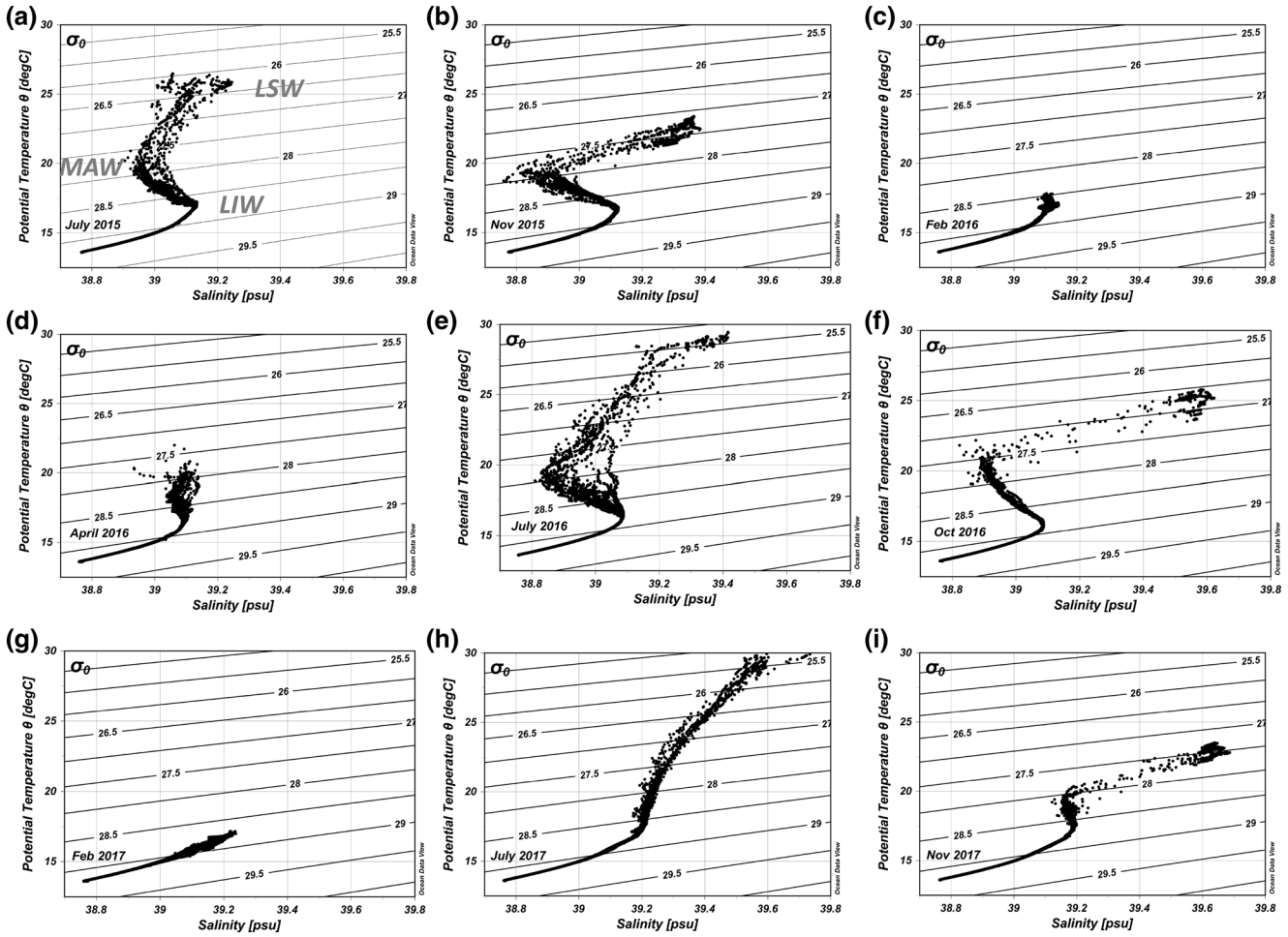

Figure 4. Potential temperature-salinity diagrams of all the Cilician Basin stations pictured in Figure 1 during the nine different cruises: (a) July2015, (b) November 2015, (c) February 2016, (d) April 2016, (e) July 2016, (f) October 2016, (g) February 2017, (h) July 2017, and (i) November 2017. Thin black lines mark isopycnals. Water masses observed are marked as LIW, Levantine Intermediate Water; LSW, Levantine Surface water; MAW, Modified Atlantic Water.

from elsewhere, either from the west or east, is mixed with the ambient water and loses its signature, or else it would have been detected.

One prominent feature of these T-S diagrams is that between 2016 and 2017 the T-S profiles are shifted to higher salinities (Figure 4). Specifically, the LIW core in October 2016 has a value of 39.09 psu and in November 2017 this value increased to 39.2 psu and temperature increased to 17.54°C (Figure 4f and 4i; Table 1). This indicates that the salinity of LIW is now 0.11 psu and temperature ~1.3°C higher than the year before. Similarly, LSW salinities in July 2015 are near 39.15 psu increasing to 39.55 psu in July 2017 (Figure 4h) and 39.66 by November 2017 (Figure 4i). This amounts to a salinity increase of ~0.5 psu in the surface waters between the 2015 and 2017 summer and fall cruises. This change in salinity is also visible when looking at the time series representation of the transect data (Figure 5) and is not likely due to be an instrumental shift, as the salinity data at deeper depths converge to identical values (Figure 4).

An abrupt increase in salinity was also reported by Hecht (1992) offshore the Israeli coast. Statistical analysis of cruise-averaged salinity profiles from 20 cruises carried out between 1979 and 1984 showed that after 1982 the average AW salinity increased by 0.15 psu, while the average LIW increased by 0.07 psu. Hecht stressed that during these cruises, the salinity and temperature at deeper levels did not change, excluding the possibility of instrument error.

The evolution of temperature, salinity, potential density anomaly, and oxygen over time (Figure 5) clearly shows the warming events during summer, intrusion of MAW between 50 and 100 m and very clearly the

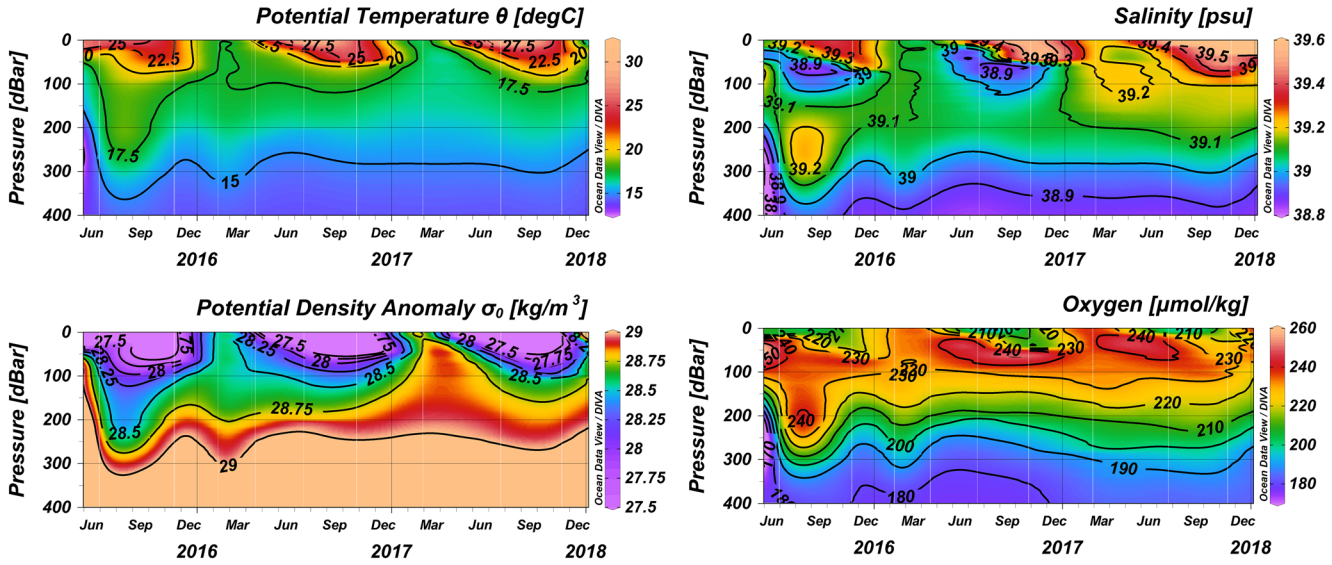

Figure 5. Time series of data from all nine cruises. Upper left: potential temperature (°C), upper right: salinity, lower left: potential density anomaly (kg/m^3), and lower right: dissolved oxygen (µmol/kg). Cruise dates are marked by white lines.

ventilation events in potential density and oxygen during the two winters 2016 and 2017 that mark the times of LIW formation.

Comparison with other studies shows that the both temperatures and salinities of the LIW in the Cilician Basin found in this study are slightly higher and densities are lower than the typical LIW values found elsewhere in the Levantine Basin (Figure 6, Table 1). These differences are likely due to the climatological conditions of the local regions where it is formed and a strong thermocline, that is, acting as a hindrance to deeper mixing. LIW in this region is generally observed at around 150–200 m which is shallower than in the Rhodes Gyre region, where it is observed at around 300–400 m (Ozsoy et al., 1989; Sur et al., 1992). LIW is found at similar depth (140–200 m) in the south-east Levantine Basin (Kress et al., 2014; Ozer et al., 2017). The variability in the depths of LIW found in the Cilician Basin is attributed to the presence of cyclonic and anticyclonic eddies. Ozsoy et al. (1989) report LIW with salinity 39.13 psu and potential temperature 16°C at 200–300 m depth in Antalya Basin; during the POPEM cruises and LIW in the Rhodes Gyre was observed at about 300 m depth with salinities of 39.06 psu and 15.5°C potential temperature, and in the southern Levantine region at 39.05 psu and 15.3°C potential temperature (Figure 6). Kucuksezgin and Pazi (2006) report LIW around 39.15 salinity and 16.2°C off to the north and east of Cyprus.

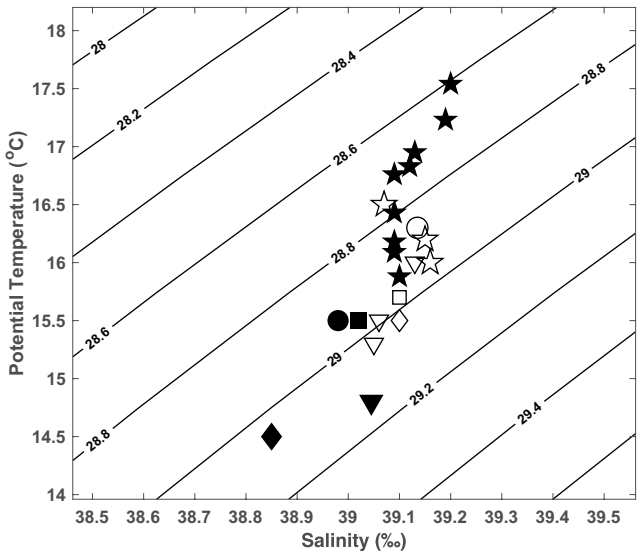

Figure 6. LIW properties from the current study (★) and historical data: Wüst (1961)—◊, Lacombe and Tchernia (1974)—□, Ozturgut (1976)—○, Ovchinnikov (1984)—▼, Plakhin and Smirnov (1984)—◊, Hecht (1986)—■, Hecht et al. (1988)—●, Ozsoy et al. (1989)—▽, Kucuksezgin and Pazi (2006)—☆.

3.3. Mesoscale Eddies and Surface Circulation

Dynamic height calculated at 10 m with reference to 500 m depth from eight of the nine cruises are used to infer the surface circulation in the study region (Figure 7). The July 2016 cruise is excluded because of insufficient data coverage of the area.

In summer 2015 (Figure 7a), the region is dominated by a southward flow between an anticyclonic eddy to the north and a cyclonic eddy in the southeast. In the next cruise, in fall 2015 these two eddies have disappeared and the region is dominated by a large cyclonic eddy (Figure 7b) of ~60–80 km diameter. In the following winter, in Febru-

Table 1
The Properties of LIW Found at the Core of LIW During all nine Cruises in the Cilician Basin

Date	Depth	Potential temperature (°C)	Salinity	Potential density (kg m^{-3})
01 July 2015	161	16.95	39.13	28.705
18 Nov 2015	176	16.83	39.12	28.717
9 Feb 2016	225	16.09	39.09	28.878
19 Apr 2016	214	16.76	39.09	28.721
20 July 2016	175	16.43	39.09	28.795
27 Oct 2016	130	16.18	39.09	28.855
27 Feb 2017	160	15.88	39.1	28.937
25 July 2017	190	17.23	39.19	28.680
16 Nov 2017	120	17.54	39.2	28.609

ary 2017 (Figure 7c), there is a region of southwesterly flow near the Turkish coast and what appears to be part of a large cyclonic eddy occupying the remaining area. April 2016 (Figure 7d) shows parts of two cyclonic eddies in the southern region. The two eddies are separated by a meandering westward flow to the north. During the following cruises, similar constellations are observed (see Figure S2) and indicate that the region is influenced by the Asia Minor current and occupied by one or more mesoscale eddies throughout the year. In the plots, the eddies are only partially defined due to the station's coverage. The presence of such mesoscale eddies in this region has also been documented in (Hecht et al., 1988; Robinson et al., 2001) and satellite data that have been compared to CTD data during the POEM program (Figure 2 in Hamad et al., 2005).

Since the dynamic height depicts the circulation in a relatively small part of the basin, satellite data of absolute dynamic topography (Figure 8) and of sea surface temperature (Figure 9) are consulted to identify the circulation features in the larger Levantine Basin area for the 2015–2016 cruises. The summer 2015 ADT (Figure 8a) and SST distribution (Figure 9a) both show a region of higher ADT and warmer water attached to the southern Turkish coast, approximately between 31°E and 34°E. There is a small region of cooler water and lower ADT just south of 36°N which extends to the northern coast of Cyprus, indicating the presence of an anticyclonic eddy. The dynamic height plot for the 2015 summer cruise (Figure 8a) shows a higher dynamic height region near the Turkish coast and part of the anticyclonic eddy. The cyclonic Rhodes Gyre is seen to extend to about 31°E. In fall 2015,

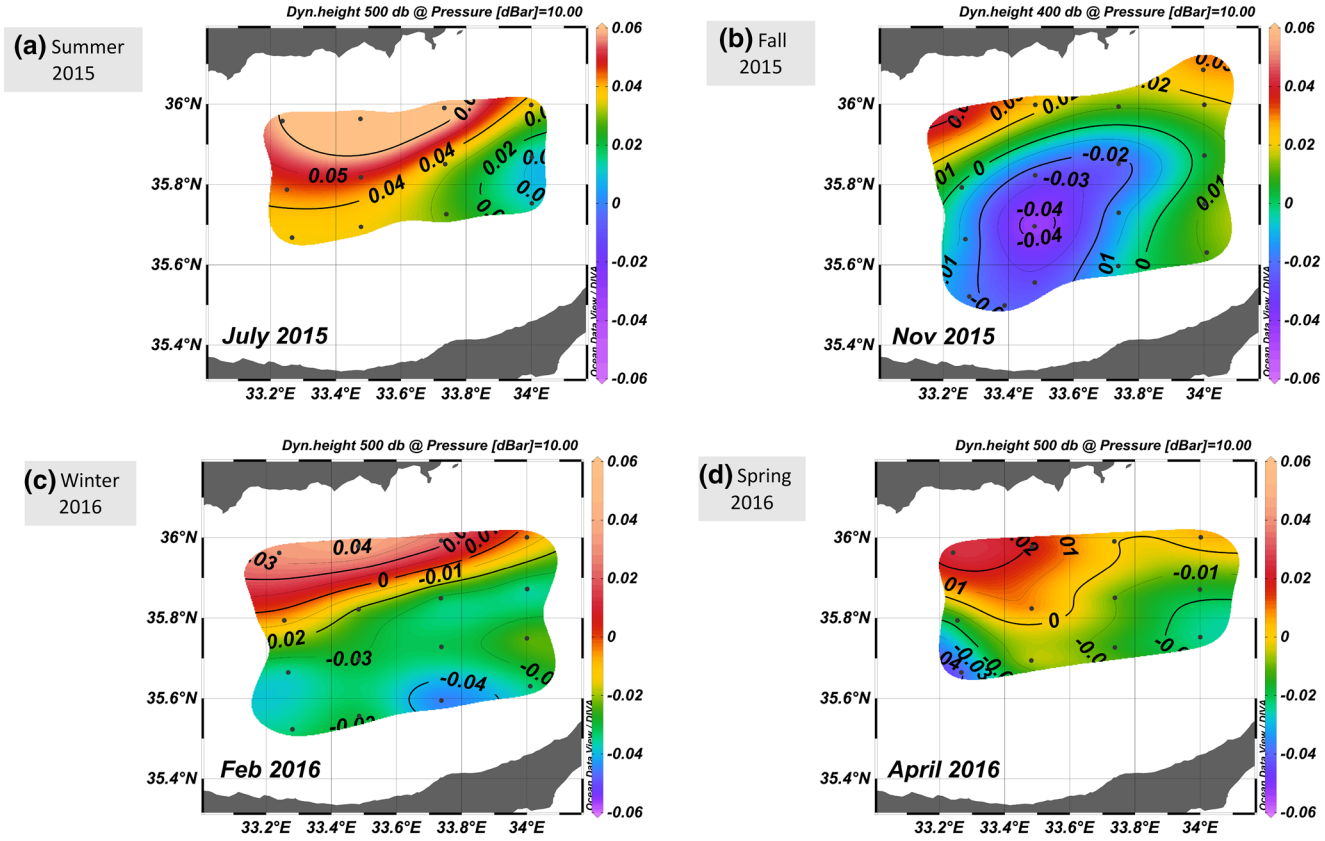

Figure 7. Dynamic height (in dynamic meters) at 10 m calculated with respect to 500 m during the first four of this study during: (a) July 2015, (b) November 2015 (calculated with respect to 400 m), (c) February 2016, and (d) April 2016.

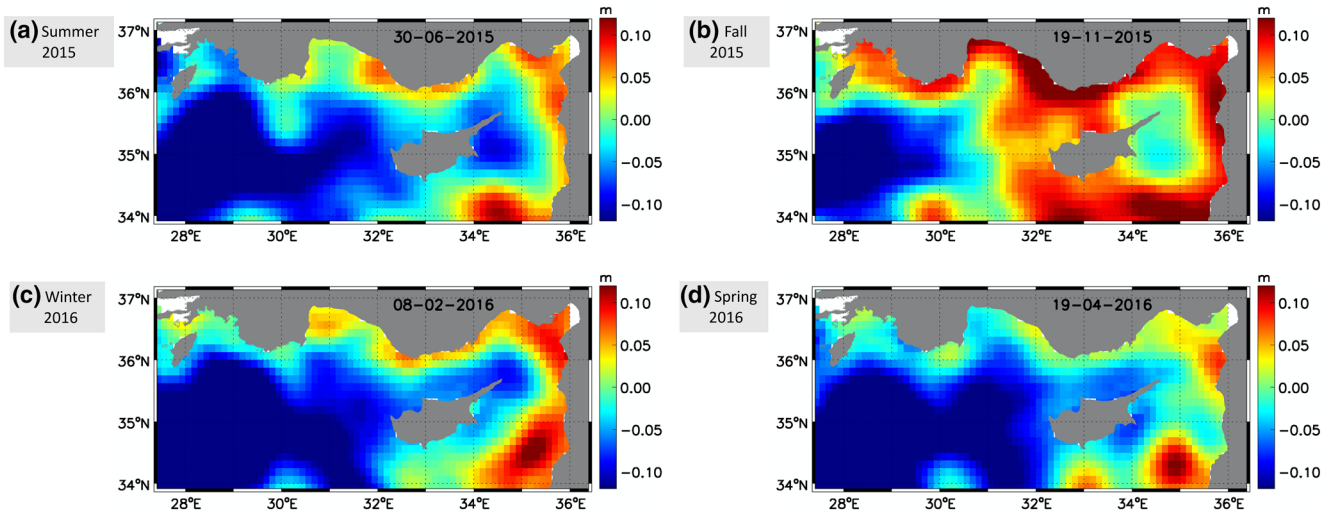

Figure 8. Daily absolute dynamic topography as derived from satellite data for the first four cruises of this study during:- (a) summer 2015, (b) fall 2015, (c) winter 2016, and (d) spring 2016. Images coincide with the exact days when cruises were undertaken.

SST shows a region of cooler water between the coasts of Turkey and Cyprus, between 33°E and 34°E, with two small regions of warmer water at the Turkish coast, approximately at 60°N (Figure 9b). The mesoscale eddies in the region have diameters of ~50–80 km. This configuration corresponds well with the dynamic height plot of the November 2015 cruise (Figure 7b). However, the ADT distribution does not show this cyclonic region in the same area, but rather places the cyclonic region further east (Figure 8a). This may possibly be because of the coarser resolution of the ADT data compared to the SST satellite data and CTD station locations. Also seen on the SST plot are the Rhodes Gyre, extending to about 31°E, an anticyclonic eddy situated at the southeast corner of Cyprus and a cyclonic eddy west of Cyprus. The mesoscale eddies observed in the region are short-lived, having a time span of a few months during which they either change location or disappear (Figures 8 and 9).

In winter 2016, the AMC is observed along the Turkish coast and a lower dynamic height region covers the rest of the area (Figure 7c). The ADT (Figure 8c) and SST data (Figure 9c) both show the same features. Rhodes Gyre extends to about 32°E, reaching the western coast of Cyprus. In spring 2016, SST data show

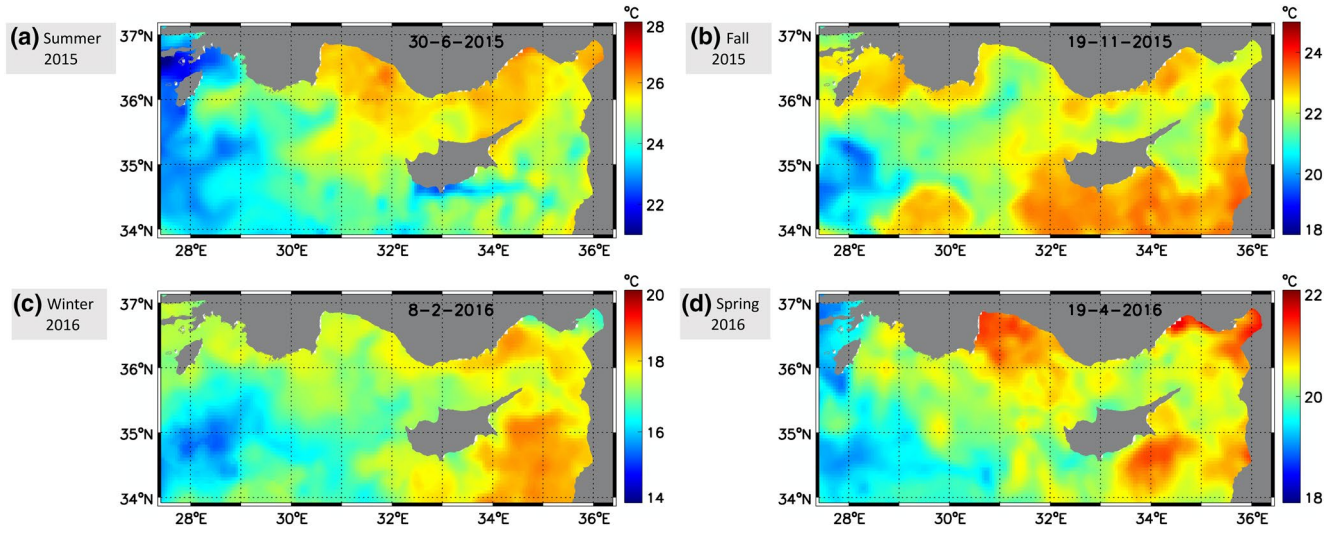

Figure 9. Daily sea surface temperature in the study region as derived from satellite data for the first four cruises of this study during: (a) summer 2015, (b) fall 2015, (c) winter 2016, and (d) spring 2016. Images coincide with the exact days when cruises were undertaken.

a mass of warm water extending southward from the Turkish coast (Figure 9d), between 33°E and 33.5°E, with cooler water masses on both sides, a situation similar to the dynamic height plot for this cruise (Figure 8d). However, a similar structure is not seen in the ADT data (Figure 9d). This may be due to the difference in resolution between data set as mentioned earlier.

3.3.1. Transport of LIW into the Region

Since the study region is located close to Rhodes Gyre, the main source of LIW in the Levantine basin, it is important to determine whether the LIW observed in the Cilician Basin is transported there from the Rhodes Gyre or if it is generated locally. Historical data from cruises covering the northern Levantine basin show that the LIW is mainly transported westwards (Malanotte-Rizzoli et al, 2003).

Data from one such cruise, carried out in November 1985 (Figure 10), show that the T-S diagram (upper left) has two branches, one with a well-defined core of LIW of salinity 38.92 psu, and a second branch with a higher core salinity of 39.04 psu. The salinity distribution (upper right) at the potential density surface 28.865 kg m^{-3}, corresponding to the lower salinity core in the upwelling Rhodes Gyre, shows that this water mass is confined to the south of about 35N. Its eastward spread, delineated by the 39 psu isohaline, is limited to the west coast of Cyprus. The dynamic height plot at 100 db referenced to 500 db clearly shows the boundary between the cyclonic Rhodes Gyre and the water mass to its northeast.

This indicates that LIW formed in the Rhodes Gyre moves south-east toward Cyprus. It does not extend eastward into the Cilician Basin, where this study takes place. This agrees with other historical data and previous studies by Lascaratos et al (1993) and Pinardi et al. (2015). Furthermore, this pattern agrees with the above discussed SST satellite data that show there is no inflow of water from the Rhodes Gyre region at the surface during any of the cruise times (Figures 9a–9d). The Cilician Basin features higher temperatures than the Rhodes Gyre area, and the cold, upwelled water from Rhodes extends south-eastward, reaching the basin south of Cyprus. This is also confirmed by other studies using satellite data investigating the extent of

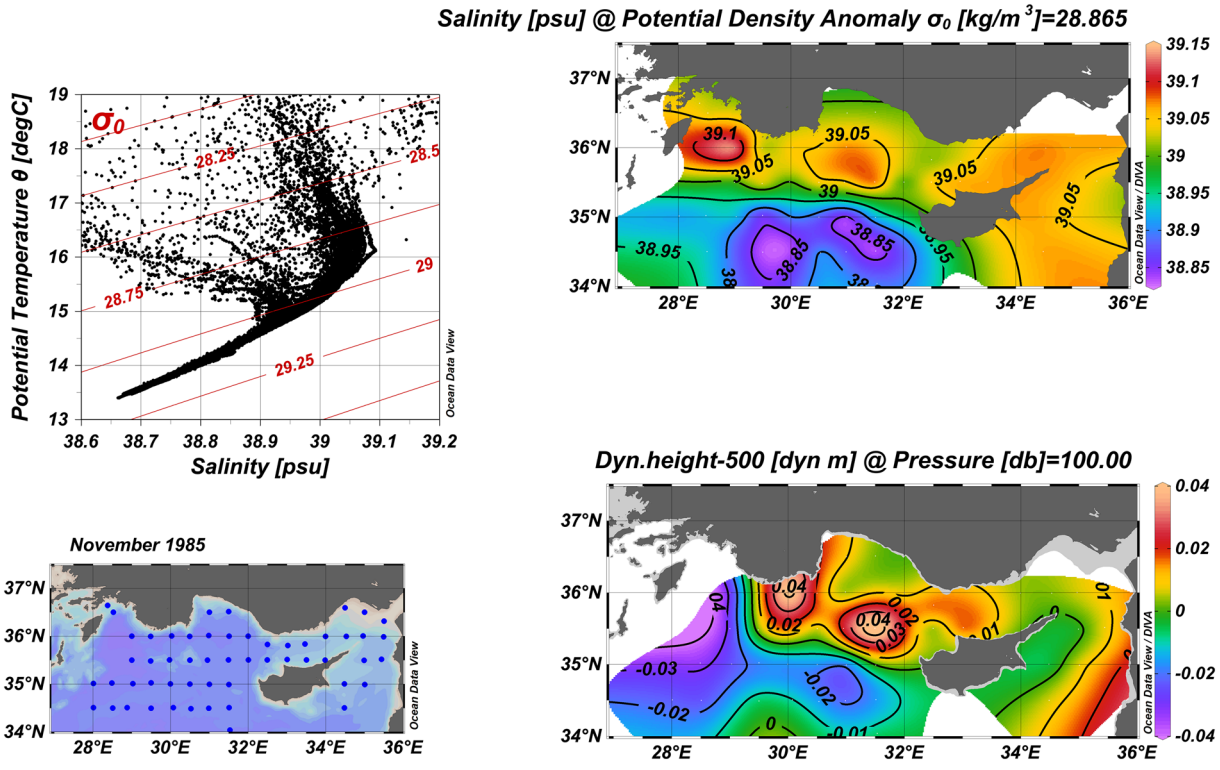

Figure 10. Historical CTD data from the November 1985 cruise of R/V Bilim 2 in the Levantine Basin with station locations (bottom left), T-S diagram (top left), salinity (top right) on the potential density surface 28.865 kg/m^3 which corresponds to the depth of LIW, and dynamic height at 100 m (bottom right).

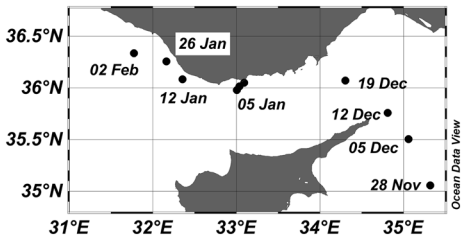

Figure 11. Pathway of Argo float 6901876 during November 2015–February 2016. Locations of the Argo float when it surfaced for data transmission are marked by filled circles and the dates are noted.

the influence of Rhodes Gyre (e.g., Hamad et al., 2005). This flow pattern has also been observed by Poulain et al. (2007) which showed a float released in the Rhodes Gyre region drifted toward south and west and not into the Cilician Basin. Hence, it is assumed here that the high salinity core of LIW detected in the Cilician Basin is not advected there directly from the Rhodes Gyre.

While a large number of Argo floats have been deployed in the Eastern Mediterranean basin, very few traversed through the study region in the same time frame. Therefore, it is not possible to supplement or directly compare the circulation patterns determined from the CTD data in this study with Argo float data. However, one float, the 6901876 ARVOR A3 profiling float, which was operational between June 2015 and February 2016, did pass through the region during the same time frame as two of the cruises conducted in this study. The float moved north initially then turned west around December 19, 2015, moving close to the Turkish coast until February 2, 2016 (Figure 11). The November 2015 and the February 2016 cruise dynamic height plots (Figure 7b and 7c) both show part of a westward current, the AMC, in the northern part of the region. Presumably the float was transported by this current. This indicates a good agreement between two independent measurements on the dynamics of the region.

3.4. Heat Flux and Buoyancy Loss

The heat flux in the study area, as calculated from ECMWF Era Interim data for the Cilician Basin, is negative between October-November through March, with values reaching a maximum of about 400–500 W/m^2 in January (Figure 12a and 12b). This heat loss is accompanied by high evaporation (Figure 12c and 12d) up to 12 mm/day as well as strong winds events (Figure 12e and 12f), resulting in the homogenous mixing that is, observed in the February cruises. The heat flux generally becomes positive at the beginning of April. These values, and the overall trend of the heat flux are similar to those reported in other studies (Hamad et al., 2006; Kubin et al., 2019; Lascaratos et al., 1993; Malanotte-Rizzoli et al., 2003; Pinardi et al., 2015).

It is important to note that short outbreaks of cold, dry air are very effective at deepening the mixed layer (Kubin et al., 2019; Malanotte-Rizzoli et al., 2003). In the time frame of 86 days, a cumulative evaporation of 473.3 mm and a 0.604 m^2/s^2 buoyancy loss in winter 2015/16 occurred in the water column (Table 2). Ninety-eight percentage of this loss was due to buoyancy loss at the surface (Table 2), and in winter 2016/17, the surface buoyancy flux contribution was 72%. This supports the conclusion that the observed high salinity core of the LIW is formed locally and not advected from other regions. It is noted that during the period of this study the peak evaporation (~12 mm/d) occurred in November each year (Figure 12), which agrees with the analysis of Matsuokas et al. (2005).

During this study, two formation periods of different length are observed in winter 2015/16 and the following winter. To estimate the rate of LIW formation and assess the importance of this region for formation in comparison to Rhodes Gyre and other regions, the rate of water mass formation is calculated for the study region following the method of Lascaratos et al. (1993). In the region of interest, which covers roughly 8,200 km^2 area, the volume of water formed in the water column of the mixed layer is divided by the formation time. Since the definition of the formation time is dependent on cruise dates and formation events may not have ended at the times of cruises or may have started earlier, it is assumed that formation takes place over an average of 90 days. This gives an approximate formation rate of ~0.3 Sv over the time frame of 3 months, or 0.1 Sv per month. It compares well with previous estimates made for the Rhodes Gyre region. Lascaratos et al. (1993) calculated a formation rate of 1 Sv over one year and Pinardi et al. (2015) estimated a 21-year monthly mean of 0.3 Sv formation in the Rhodes Gyre Region.

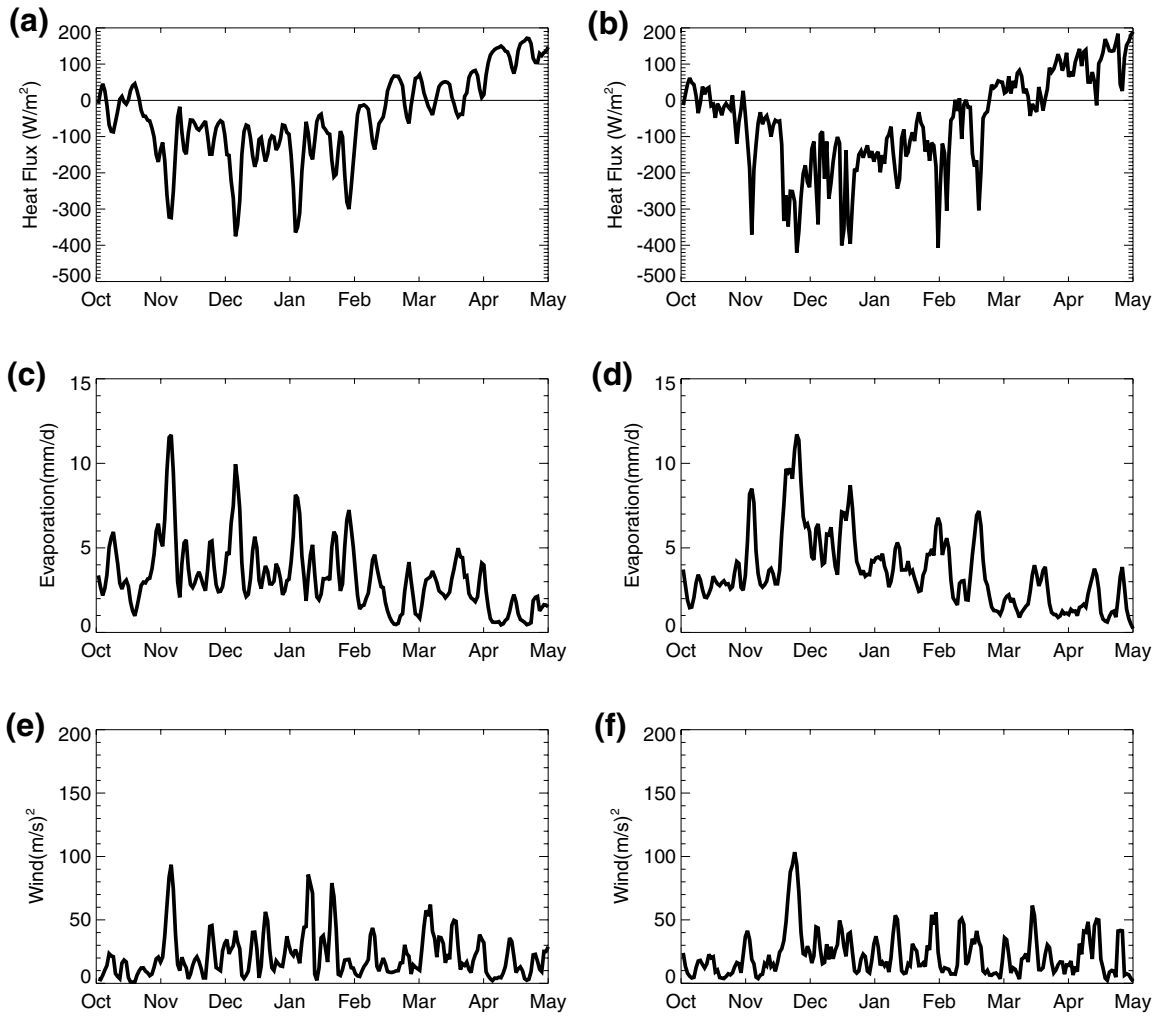

Figure 12. Sea surface heat flux (Wm^{-2}) in (a) winter 2015–2016 and (b) winter 2016–2017, evaporation (mm/d) in (c) winter 2015–2016 and (d) winter 2016–2017 and wind speed $(m/s)^2$ in (e) winter 2015–2016 and (f) calculated from ECMWF Era Interim data (see Figure 1 for location). Thin line in A and B marks zero heat flux.

Table 2
Changes in Buoyancy Content From CTD and Meteorological Data (ECMWF) During LIW Formation Times

Dates (CTD stations)	Duration (days)	Change in buoyancy content from CTD data (m^2/s^2)	Total surface buoyancy flux from meteorological data (m^2/s^2)	E-P (mm/d)	Mixed layer depth (m)
18 Nov 2015–9 Feb 2016	83	−0.604	−0.594	473.3	200
27 Oct 2016–28 Feb 2017	126	−1.286	−0.933	451.8	200

4. Discussion

4.1. Water Mass Properties

The present study focused on temporal variations of the Cilician Basin water mass properties and oceanographic conditions. Previous hydrographic studies in the Levantine Basin, such as the POEM cruises, encompassed a much larger region, and helped to understand the general state of the north-eastern Levantine Basin. In this study with nine cruises in 2.5 years, seasonal changes in the water mass properties were more closely followed, as seen in the T-S diagrams (Figure 4).

The data collected show a typical annual cycle of temperature and salinity changes, related with seasonal climate variations. In the 2.5 years period of the duration of the study, the water column consistently became uniformly homogeneous from the surface to a depth of about 250 m in winter. Subsequently, in the following months, LIW was observed at depths between 150 and 200 m, while MAW was observed at ~50 m. Below the LIW, at ~800–1000 m, the beginning of deep water of the EMDW was located during all cruises.

It was determined that the Cilician Basin is also a formation region of LIW. In winter, strong mixing of the water column to about 250 m depth is observed, creating dense, saline water of the typical LIW characteristics (salinity 39.1–39.2, potential temperature ~16°C, and potential density of 28.8 kg/m^3) in the Cilician Basin. In subsequent spring and summer cruises, LIW appears centered at ~200m depths. Using ECMWF climatological data, it is found that about 70%–98% of the buoyancy loss in the water column results from buoyancy loss due to surface fluxes. This surface buoyancy loss is in agreement with the findings of LIWEX that showed formation of LIW in the Rhodes Gyre region (Malanotte-Rizzoli et al., 2003).

It was shown from satellite SST (Figure 9) and historical CTD data (Figure 10) that there is no transport of LIW from the Rhodes Gyre region eastward into the Cilician Basin. This is inferred from the fact that water from the Rhodes Gyre region spreads south-eastward to the south of Cyprus. LIW formed in previous years could be transported to the Cilician Basin from the east via the AMC indicating a transport all the way from south of Cyprus. However, the high salinity core of LIW is not observed in the water column mixed down to ~250 m in winter, indicating that any water mass transported into the region becomes mixed with the ambient water or else it would have been detected. Therefore, the high salinity core of the LIW observed in the Cilician Basin is most probably formed locally. This is significant in that it adds to the amount of LIW water formed in the Levantine Basin, which has wide reaching implications since the LIW reaches as far as the Atlantic Ocean.

One other interesting result is the observed increase in salinity of both LSW and in the LIW core in the 2017 cruises covering winter, summer and fall seasons (Figures 4 and 5). The deeper layers, below 800 m, however showed no changes in salinity over the 2.5-year period of the study (Figure 4). The salinity of LIW increased by ~0.11 psu, while the surface water salinity increased by ~0.5 psu. MAW showed a larger range of salinity values before 2017 than the other water masses, but also for that water mass an increase in salinity is observed. When compared to historical data of the POEM cruises, where surface salinities stayed well below 39.1 (Figure 10), this is a rather large increase. As these both are snapshots of different time frames 30 years apart, it is not clear how surface waters developed over this time frame. However, 2017 has been a high salinity year elsewhere in the Mediterranean, such as in the Cretan Passage and the south of the Ionian Sea (Grodkya et al., 2019).

Increases in surface salinity values have previously been observed in the Eastern Mediterranean and identified by Ozer et al. (2017) as a trend of +0.008 per year over 30 years in LSW and LIW masses in the south-eastern Mediterannean. This trend has been explained with changes in the water budget (increases in E-P) (Mariotti, 2010; Skliris et al., 2018) or changes in wind patterns and regional circulation (Demirov & Pinardi, 2002) and is also affected by the transport of water masses such as the MAW across the Mediterranean (Font et al., 1998). Also, a shift of the North Ionian Gyre from cyclonic to anticyclonic circulation, that is, bringing more salty water into the northern Levantine Basin (Borzelli et al., 2009) due to the Bimodal Oscillating system (BiOS) controlling the trajectory of the MAW flow after passing through the Sicily Straits to both the Southern Adriatic and the Levantine Basin can be one explanation for increased salinity (Gač;ić et al., 2011); they showed that the North Ionian Gyre (NIG) flow can reverse from cyclonic to anticyclonic and vice versa. During cyclonic NIG, the surface salinity in the Southern Adriatic increases and in the Levantine Basin decreases and vise-versa for anticyclonic NIG. Recently, Kassis and Korres (2020) found positive trends of temperature and salinity that exceed 0.06 C and 0.02 psu in the years 2012–2017 at the intermediate, and deep layers from Argo float data of the eastern Mediterranean. Furthermore, Grodsky et al (2019) observed a salinification of the Levantine Basin at a rate of ~0.14 psu/year during the years 2015–2018 with satellite sea surface salinity data complemented with Argo data, which are comparable to the observations of this study. They conclude that this sea surface salinization occurs due to a shift in the abovementioned BiOS pattern that decreases the freshwater transport to the Levantine Basin. The effect of this shift was amplified by a strengthening of local winds that increased evaporative losses and weakened cyclonic currents in the eastern Mediterranean in connection to the NAO atmospheric pressure pattern. The

reason for the salinity shift in the Cilician Basin observed in this study cannot be determined with the data collected in this study, however it should be further investigated in future studies.

4.2. LIW Formation, Transport, Rate of Formation

The findings of this study indicate another region of LIW water formation in the Cilician Basin in addition to the main Rhodes Gyre. Other locations along the southern coast of Turkey where LIW formation was observed have also been identified (Kubin et al., 2019; Sur et al., 1992). The LIW produced in the Cilician Basin has temperatures and salinities that are slightly higher and hence densities that are lower than the typical LIW (potential temperature > 16.4°C and salinity > 39.1) (Figure 6). There are, in fact, no fixed values for the LIW properties; a range of temperature and salinities exists for the LIW, depending on the location and climatological conditions as reported in different regions of the Levantine basin (Kubin et al., 2019; Kucuksezgin & Pazi, 2006; Ozsoy et al., 1989; Sur et al., 1992).

Intermediate water mass formation is an important process occurring in the Mediterranean Sea. At present, our knowledge of water mass formation rates is based mainly on model results (Lascaratos et al., 1993; Nittis & Lascaratos, 1998; Pinardi et al., 2015). The present study provides a measured, although an approximate, estimate of ∼0.3 Sv over the time frame of 3 months as the formation rate in the region studied. As the study area is small compared to the main region of LIW formation in the Rhodes gyre, it is not surprising that the LIW formation rate calculated for the Rhodes Gyre of 0.7 and 1 Sv (Nittis & Lascaratos, 1998, and references therein) and a typical climatological value of ∼1.0 Sv (Lascaratos et al., 1993) are higher than the rate calculated in this study.

4.3. Mesoscale Eddies

The dynamic height plots of the seasonal cruises show the presence of one or more meso-scale eddies for the first time in the study area throughout the year (Figure 7 and Figure S2). These eddies have a diameter of ∼50–80 km, which is in agreement with mesoscale eddies previously observed in the Levantine Basin (Robinson et al., 2001). Their horizontal scale is related to the internal Rossby radius of deformation which is 10–14 km in the Mediterranean Sea. Even though in some cruises the data show only partial eddies due to lack of station coverage, satellite data (Figures 8 and 9) and other studies (Hamad et al., 2005; Hecht et al., 1988; Robinson et al., 2001) show that they are complete cyclonic and anticyclonic eddies. These eddies are observed to be short-lived in this study, having a life span of only a few months, during which they either change location or disappear from cruise to cruise.

This is in agreement with previous studies (Hamad et al., 2006; Mauri et al., 2019; Ozsoy et al., 1989; Robinson et al., 2001) that report rapid changes in the eddy dynamics in the Levantine Basin, but contrary to Hecht et al. (1988) who found the time scale of the persistence of the eddies varies between 6 months and a year in the southern Levantine Basin. They find that eddies there are almost stationary but undergo changes in strength and shape. In the Cilician Basin however, the situation is rather different as eddies are constrained between two coasts and are being propelled by the AMC which may be one reason for their variability.

5. Conclusion

In this study, the seasonal variability of water masses in the Cilician Basin, north-eastern Levantine Basin was studied over the course of 2.5 years with nine seasonal cruises. This study has shown for the first time that the Cilician Basin is another region of LIW formation in addition to the Rhodes Gyre, where about 10% of the total LIW produced in the main formation region, Rhodes Gyre, may be formed. The local processes in the Cilician Basin are therefore of importance for water masses in the entire Mediterranean and beyond in the Atlantic Ocean. In this study, many eddies were observed in the region that were found to be short-lived (a few months) during which they either changed location or completely disappeared. The location of the Cilician Basin between two land masses causes eddies to be constrained between the two coasts and being moved along by the AMC. The effect of these eddies on water masses are linked to cyclonic eddies being upwelling and anticyclonic eddies being downwelling areas, in which water masses will either be moved deeper or higher than in the surrounding water.

In addition, a significant increase in salinity of LSW and LIW has been found in this study for the year 2017 for which the reasons should be investigated in future studies. Possible reasons to be investigated for this increase can be changes in heat fluxes and evaporation rates over the past decades, changes in water masses transported by the Asia Minor Current, reduced river inflow into the Eastern Mediterranean, as well as the influence of the Bimodal Oscillating system and wind patterns. The process of water mass formation and also the observed increase in salinity of LIW and LSW have implications for the ecosystem in the Cilician Basin, such as on nutrient and oxygen concentrations which should be further investigated. The data and analysis presented in this study provide a valuable time-series to interpret ongoing changes in deep water formation in the north-eastern Levantine Basin.

Data Available Statement

The data used in this publication are available at SeaDataNet, Pan-European Infrastructure for ocean & marine data management (https://cdi.seadatanet.org/search) under the data identifier "DEKOSIM_KIBRIS." The Ocean Data View software was used to draw some of the figures (Schlitzer, R., Ocean Data View, https://odv.awi.de, 2020.)

Acknowledgments
This research was funded by the Turkish Scientific and Technical Council (TÜBİTAK) Project No: 114Y139. The authors acknowledge support by DEKOSIM (BAP-08-11-DPT2012K120880) funded by the Turkish Ministry of Development. Dr. Bettina Fach acknowledges support by the TÜBİTAK Project No: 117Y396.

References

Akbulut, N. E., Şahin, Y., Bayari, S., & Akbulut, A. (2009). The rivers of Turkey. In K. Tockner, U. Uehlinger, & C. T. Robinson (Eds.), *Rivers of Europe* (pp. 643–672). Academic Press. https://doi.org/10.1016/B978-0-12-369449-2.00017-5

Borzelli, G. L. E., Gačić, M., Cardin, V., & Civitarese, G. (2009). Eastern Mediterranean transient and reversal of the Ionian Sea circulation. *Geophysical Research Letters*, *36*, L15108. https://doi.org/10.1029/2009GL039261

Carpenter, J. H. (1965). The Chesapeake Bay institute technique for the Winkler dissolved oxygen method. *Limnology and Oceanography*, *10*, 141–143. https://doi.org/10.4319/lo.1965.10.1.0141

Demirov, E., & Pinardi, N. (2002). Simulation of the Mediterranean Sea circulation from 1979 to 1993: Part I. the interannual variability. *Journal of Marine Systems*, *33–34*, 23–50. https://doi.org/10.1016/S0924-7963(02)00051-9

Ediger, V., Ergin, M., & Ediger, V.. (1997). Transportation of coniferous bisaccate pollen from land to sea and deposition along the shelf off Erdemli (Turkey), NE-Mediterranean Sea. *Bolletino Di Geofisica Teorica Ed Applicata*, *38*(3–4), 307–321.

Font, J., Millot, C., Salas, J., Juliá, A., & Chic, O. (1998). The drift of modified Atlantic water from the Alboran Sea to the eastern Mediterranean. *Scientia Marina*, *62*, 211–216. https://doi.org/10.3989/scimar.1998.62n3211

Gačić, M., Civitarese, G., Eusebi Borzelli, G. L., Kovačević, V., Poulain, P.-M., Theocharis, A., et al. (2011). On the relationship between the decadal oscillations of the northern Ionian Sea and the salinity distributions in the eastern Mediterranean. *Journal of Geophysical Research*, *116*, C12002. https://doi.org/10.1029/2011JC007280

Grodskya, S. A., Reul, N., Bentamy, A., Vandemark, D., & Guimbard, S. (2019). Eastern Mediterranean salinification observed in satellite salinity from SMAP mission. *Journal of Marine Systems*, *198*, 103190. https://doi.org/10.1016/j.jmarsys.2019.103190

Hamad, N., Millot, C., & Taupier-Letage, I. (2005). A new hypothesis about the surface circulation in the eastern basin of the Mediterranean Sea. *Progress in Oceanography*, *66*, 287–298.

Hamad, N., Millot, C., & Taupier-Letage, I. (2006). The surface circulation in the eastern basin of the Mediterranean Sea. *Scientia Marina*, *70*(3), 457–503.

Hecht, A. (1992). Abrupt changes in the characteristics of Atlantic and Levantine intermediate waters in the Southeastern Levantine basin. *Oceanologica Acta*, *15*(1), 25–42.

Hecht, A., Pinardi, N., & Robinson, A. R. (1988). Currents, water masses, eddies and jets in the Mediterranean Levantine Basin. *Journal of Physical Oceanography*, *18*(10), 1320–1353.

Kassis, D., & Korres, G. (2020). Hydrography of the Eastern Mediterranean basin derived from argo floats profile data. *Deep-Sea Research Part II*, *171*, 104712. https://doi.org/10.1016/j.dsr2.2019.104712

Kress, N., Gertman, I., & Herut, B. (2014). Temporal evolution of physical and chemical characteristics of the water column in the Easternmost Levantine basin (Eastern Mediterranean Sea) from 2002 to 2010. *Journal of Marine System*, *135*, 6–13.

Kubin, E., Poulain, P.-M., Mauri, E., Menna, M., & Notarstefano, G. (2019). Levantine Intermediate and Levantine Deep Water Formation: An Argo Float Study from 2001 to 2017. *Water*, *11*, 1781. https://doi.org/10.3390/w11091781

Kucuksezgin, F., & Pazi, I. (2006). Circulation, hydrographic and nutrient characteristics of the Cilician Basin, Northeastern Mediterranean Sea. *Journal of Marine Systems*, *59*(3–4), 189–200.

Lacombe, H., & Tcherina, P. (1974). *Hydrography of the Mediterranean, consultation on the protection of living resources and fisheries from pollution in the Mediterranean, FAO*. Rome, Italy: FlD;PPM/73/Inf.3.

Lascaratos, A., Williams, R. G., & Tragou, E. (1993). A mixed-layer study of the formation of Levantine intermediate water. *Journal of Geophysical Research*, *98*, 14739. https://doi.org/10.1029/93JC00912

Lazar, A. (2019). *Intermediate dense water formation and current variability in the southeastern Levantine basin from the DeepLev moored station and gliders*. San Francisco: American Geophysical Union.

Malanotte-Rizzoli, P., Artale, V., Borzelli-Eusebi, G. L., Brenner, S., Crise, A., Gacic, M., et al. (2014). Physical forcing and physical/biochemical variability of the Mediterranean Sea: A review of unresolved issues and directions for future research. *Ocean Science*, *10*, 281–322.

Malanotte-Rizzoli, P., & Bergamasco, A. (1989). The General Circulation of the Eastern Mediterranean, Part I: The Barotropic, Wind Driven Circulation. *Oceanologica Acta*, *12*, 335–351.

Malanotte-Rizzoli, P., & Hecht, A. (1988). Large- scale properties of the eastern Mediterranean: A review. *Oceanologica Acta*, *11*, 323–335.

Malanotte-Rizzoli, P., Manca, B. B., Marullo, S., Ribera d'Alcalà, M., Roether, W., Theocharis, A., et al. (2003). The LIWEX group: The Levantine Intermediate Water Experiment, the Levantine basin as a laboratory for multiple water mass formation processes,. *Journal of Geophysical Research*, *9*, 8101. https://doi.org/10.1029/2002JC001643

Malanotte-Rizzoli, P., Manca, B. B., Ribera d'Alcala, M., Theocharis, A., Brenner, S., Budillon, G., et al. (1999). The Eastern Mediterranean in the 80s and in the 90s: The big transition in the intermediate and deep circulations. *Dynamics of Atmospheres and Oceans*, *29*(2–4), 365–395. https://doi.org/10.1016/S0377-0265(99)00011-1

Manca, B., Burca, M., Giorgetti, A., Coatanoan, C., Garcia, M.-J., & Iona, A. (2004). Physical and biochemical averaged vertical profiles in the Mediterranean regions: An important tool to trace the climatology of water masses and to validate incoming data from operational oceanography. *Journal of Marine Systems*, *48*, 83–116.

Mariotti, A. (2010). Recent changes in the Mediterranean water cycle: A pathway toward long-term regional hydroclimatic change? *Journal of Climate*, *23*, 1513–1525. https://doi.org/10.1175/2009JCLI3251.1

Mariotti, A., Struglia, M. V., Zeng, N., & Lau, K. M. (2002). The hydrological cycle in the mediterranean region and implications for the water budget of the mediterranean sea. *Journal of Climate*, *15*, 1674–1690. https://doi.org/10.1175/15200442(2002)015<1674:thcitm>2.0.co;2

Matsoukas, C., Banks, A. C., Hatzianastassiou, N., Pavlakis, K. G., Hatzidimitriou, D., Drakakis, E., et al. (2005). Seasonal heat budget of the Mediterranean Sea. *Journal of Geophysical Research*, *110*, C12008. https://doi.org/10.1029/2004JC002566

Mauri, E., Sitz, L., Gerin, R., Poulain, P.-M., Hayes, D., & Gildor, H. (2019). On the variability of the circulation and Water Mass Properties in the Eastern Levantine Sea between September 2016–August 2017. *Water*, *11*, 1741. https://doi.org/10.3390/w11091741

Mertens, C., & Schott, F. (1998). Interannual variability of deep-water formation in the northwestern Mediterranean. *Journal of Physical Oceanography*, *28*, 1410–1424.

Morcos, S. A. (1972). Sources of Mediterranean intermediate water in the Levantine Sea. In A. L. Gordon (Ed.), *Studies in physical oceanography* (*2*, pp. 185–206). New York, NY: Gordon & Breach.

Nittis, K., & Lascaratos, A. (1998). Diagnostic and prognostic numerical studies of LIW formation. *Journal of Marine Systems*, *18*, 179–195.

Ovchinnikov, I. M. (1984). The formation of Intermediate Water in the Mediterranean. *Oceanology*, *24*(2), 168–173.

Ozer, T., Gertman, I., Kress, N., Silverman, J., & Herut, B. (2017). Interannual thermohaline (1979–2014) and nutrient (2002–2014) dynamics in the Levantine surface and intermediate water masses, SE Mediterranean Sea. *Global and Planetary Change*, *151*, 60–67. https://doi.org/10.1016/j.gloplacha.2016.04.001

Ozsoy, E. (1981). On the atmospheric factors affecting the Levantine sea, European Centre for Medium Range Weather Forecasts. Reading, UK, Technical Report 25, 29 p.

Ozsoy, E., Hecht, A., & Unluata, U. (1989). Circulation and hydrography of the Levantine Basin. Results of POEM coordinated experiments 1985-1986. *Progress in Oceanography*, 90004–90009. http://doi.org/10.1016/0079-6611(89)90004-9

Ozsoy, E., Hecht, A., Unluata, U., Brenner, S., Oguz, T., Bishop, J., et al. (1991). A review of the Levantine Basin circulation and its variability during 1985-1988. *Dynamics of Atmospheres and Oceans*, *15*(3–5), 421–456. http://doi.org/10.1016/0377-0265(91)90027-D

Ozsoy, E., Hecht, A., Unluata, U., Brenner, S., Sur, H. I., Bishop, J., et al. (1993). A synthesis of the Levantine Basin circulation and hydrography, 1985-1990. *Deep-Sea Research Part II*, *40*(6), 1075–1119. http://doi.org/10.1016/0967-0645(93)90063-S

Ozturgut, E. (1976). *The source and spreading of the levantine intermediate water in the eastern mediterranean* (p. 45). La Spezia, Italy: Memor. SM-92. Saclant ASW Research Center.

Pinardi, N., & Masetti, E. (2000). Variability of the large scale general circulation of the Mediterranean Sea from observations and modelling: A review. *Palaeogeography, Palaeoclimatology, Palaeoecology*, *158*, 153–173.

Pinardi, N., Zavatarelli, M., Adani, M., Coppini, G., Fratianni, C., Oddo, P., et al. (2015). Mediterranean Sea large-scale low-frequency ocean variability and water mass formation rates from 1987 to 2007: A retrospective analysis. *Progress in Oceanography*, *132*, 318–332. https://doi.org/10.1016/j.pocean.2013.11.003

Plakhin, E. A., & Smirnov, V. G. (1984). Determination of initial T, S indices of the Mediterranean Waters. *Oceanology*, *24*(2), 226–230.

Poulain, P.-M., Barbanti, R., Font, J., Cruzado, A., Millot, C., Gertman, I., et al. (2007). MedArgo: A drifting profile program in the Mediterranean Sea. *Ocean Science*, *3*, 379–395.

Robinson, A. R., Leslie, W. G., Theocharis, A., & Lascaratos, A. (2001). In J. H. Steele S. A. Thorpe & K. K. Turekian (Eds.). *Mediterranean Sea circulation, encyclopedia of ocean Sciences* (pp. 1689–1706). Academic Press.

Robinson, A. R., Malanotte-Rizzoli, P., Hecht, A., Michelato, A., Roether, W., Theocharis, A., et al. (1992). General circulation of the eastern mediterranean. *Earth-Science Reviews*, *32*, 285–309. https://doi.org/10.1016/0012-8252(92)90002-B

Sannino, G., Sánchez Garrido, J. C., Liberti, L., & Pratt, L. (2014). Exchange Flow through the Strait of Gibraltar as Simulated by a σ-Coordinate Hydrostatic Model and a z-Coordinate Nonhydrostatic Model. In G. Eusebi Borzelli, M. Gačić, P. Lionello, & P. Malanotte-Rizzoli (Eds.). *The Mediterranean Sea: Temporal variability and spatial patterns*. American Geophysical Union. https://doi.org/10.1002/9781118847572.ch3

Skliris, N., Zika, J. D., Herold, L., Josey, S. A., & Marsh, R. (2018). Mediterranean Sea water budget long-term trend inferred from salinity observations. *Climate Dynamics*, *51*, 2857–2876. https://doi.org/10.1007/s00382-017-4053-7

Sur, H., Ozsoy, E., & Unluata, U. (1992). Simultaneous deep and intermediate depth convection in the northern levantine sea, winter 1992. *Oceanologica Acta*, *16*(1), 33–43.

Tanhua, T., Hainbucher, D., Schroeder, K., Cardin, V., Alvarez, M., & Civitarese, G. (2013). The Mediterranean Sea system: A review and an introduction to the special issue. *Ocean Science*, *9*, 789–803. http://dx.doi.org/10.5194/os-9-789-2013

Waldman, R., Brüggemann, N., Bosse, A., Spall, M., Somot, S., & Sevault, F. (2018). Overturning the Mediterranean thermohaline circulation. *Geophysical Research Letters*, *45*, 8407–8415. https://doi.org/10.1029/2018GL078502

Wu, P., & Haines, K. (1998). The general circulation of the Mediterranean Sea from a 100-year simulation. *Journal of Geophysical Research*, *103*(C1), 1121. http://doi.org/10.1029/97JC02720

Wüst, G. (1961). On the vertical circulation of the Mediterranean Sea. *Journal of Geophysical Research*, *66*(10), 3261. http://doi.org/10.1029/JZ066i010p03261

Zahariev, K., & Garrett, C. (1997). An apparent surface buoyancy flux associated with the non-linearity of the equation of state. *Journal of Physical Oceanography*, *27*, 362–368.